Properties of the one-particle-displacement probability distribution in systems undergoing antiferrodistortive structural phase transitions

T. Schneider and E. Stoll
IBM Zurich Research Laboratory, 8003 Rüschlikon, Switzerland
(Received 25 February 1974)

Using the Hartree approximation, a high-temperature expansion, and the molecular-dynamics technique, we study some properties of the one-particle probability distribution $F_1(U_x^{\vec{1}})$ of the displacement U_x of particle one in a model system. The system is two dimensional and subjected to constraints in such a way that it exhibits antiferrodistortive structural phase transitions. It covers the displacive and order-disorder regime, including the Ising and displacive limit. We present evidence that $F_1(U_x^{\vec{1}})$ or its symmetrized analog $\tilde{F}_1(U_x^{\vec{1}}) = \frac{1}{2}[F_1(U_x^{\vec{1}}) + F_1(-U_x^{\vec{1}})]$, being a very useful property to elucidate the regime to which a particular antiferrodistortive transition belongs. In the displacive regime, the ratio

$$a_s = \left(\frac{d}{dU_x^{\vec{1}}}\tilde{F}_1(U_x^{\vec{1}})\right)_{\max} \Big/ \left(\frac{d}{dU_x^{\vec{1}}}\tilde{F}_1(U_x^{\vec{1}})\right)_{\min},$$

for $U_x^{\vec{1}}$ either negative or positive, is shown to diverge at some temperature T^*, because $\tilde{F}_1(U_x^{\vec{1}})$ exhibits for $T < T^*$ a double-peak structure disappearing at $T = T^*$. In the order-disorder regime, the ratio T^*/T_c is infinite and decreases in the displacive regime by approaching the displacive limit to some value $T^*/T_c < 1$. As Müller and Berlinger have shown, the key quantity a_s can be measured, close to T_c, by means of the electron-paramagnetic-resonance technique.

I. INTRODUCTION

In this work, we study some properties of the one-particle probability distribution $F_1(U_x^{\vec{1}})$ of the displacement $U_x^{\vec{1}}$ of particle one in a two-dimensional model system. The system is subjected to constraints so that it exhibits antiferrodistortive-structural-phase transitions. It covers the order-disorder and the displacive regime, including the Ising and the displacive limit.

Recently, we also performed a molecular-dynamics study of static and dynamic properties of this model system.[1,2] It was shown, as expected from the universality hypothesis, that the critical exponents β and γ are consistent with $\beta = \frac{1}{8}$ and $\gamma = \frac{7}{4}$, the exponents of the two-dimensional Ising model. Moreover, we elucidated the microscopic origin of the central-peak phenomenon, occurring close to T_c, in the dynamic form factor of the density fluctuations. This work demonstrated the formation of clusters in such a system consisting of particles with a spontaneous local-order parameter contrary to that expected from zero temperature. Moreover, it was shown that these clusters increase in size by approaching T_c, so that a slowing down of their dynamics occurs, giving rise to the central-peak phenomenon, first observed in $SrTiO_3$ by means of the neutron-scattering technique.[3,4] It should be noted that the existence of correlated regions (clusters) has been inferred[5] from the anisotropy of the electron-paramagnetic (EPR) linewidth in $SrTiO_3$.

The present work was mainly motivated by the EPR study of $\tilde{F}_1(U_x^{\vec{1}}) = \frac{1}{2}[F_1(U_x^{\vec{1}}) + F_1(-U_x^{\vec{1}})]$ in $SrTiO_3$, by Müller and Berlinger.[6] These authors demonstrated that $\tilde{F}_1(U_x^{\vec{1}})$ can be measured very accurately close to T_c and, moreover, that the ratio

$$\left(\frac{d}{dU_x^{\vec{1}}}\tilde{F}_1(U_x^{\vec{1}})\right)_{\max} \Big/ \left(\frac{d}{dU_x^{\vec{1}}}\tilde{F}_1(U_x^{\vec{1}})\right)_{\min}$$

tends to diverge, at least in $SrTiO_3$, close to T_c.

In Sec. II, we characterize the model system. Section III is devoted to sketching a mathematical formalism, developed in the context of the theory of classical liquids,[7] which constitutes a convenient basis to investigate the properties of $\tilde{F}_1(U_x^{\vec{1}})$ and $F_1(U_x^{\vec{1}})$. In Sec. IV, we study these properties within the framework of the Hartree approximation, in Sec. V by means of a high-temperature expansion, and finally, in Sec. VI, by means of the molecular-dynamics results. The main results will be summarized in Sec. VI. They include the following points: Conclusive evidence is given that the one-particle probability distributions, $F_1(U_x^{\vec{1}})$ or $\tilde{F}_1(U_x^{\vec{1}})$ are very useful properties to elucidate the regime to which a particular antiferrodistortive transition belongs. Moreover, it is shown that the divergence of the ratio

$$\left(\frac{d}{dU_x^{\vec{1}}}\tilde{F}_1(U_x^{\vec{1}})\right)_{\max} \Big/ \left(\frac{d}{dU_x^{\vec{1}}}\tilde{F}_1(U_x^{\vec{1}})\right)_{\min}$$

is noncritical in nature, but a property of the displacive regime.

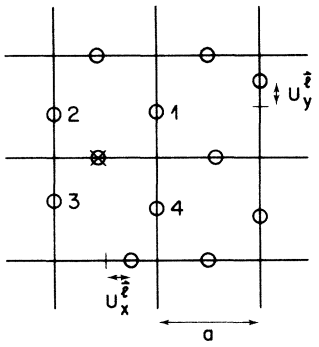

FIG. 1. Arrangement of the particles in the reference-square lattice with lattice constant a and two atoms per cell. 1, 2, 3 and 4 label the nearest neighbors of the particle marked by ⊠.

II. MODEL SYSTEM

A two-dimensional model Hamiltonian, covering the whole range from the order-disorder limit to the displacive limit, reads[1,2,8]

$$\mathcal{H} = T + V , \tag{1}$$

$$T = \sum_{\vec{l}} (P_x^{\vec{l}})^2 + (P_y^{\vec{l}})^2, \tag{2}$$

$$V = V_s + V_I , \tag{3}$$

$$V_s = \tfrac{1}{2}A\sum_{\vec{l}} [(U_x^{\vec{l}})^2 + (U_y^{\vec{l}})^2] + \tfrac{1}{4}B \sum_{\vec{l}} [(U_x^{\vec{l}})^4 + (U_y^{\vec{l}})^4] \tag{4}$$

$$V_I = \sum_{\vec{l},\vec{l}'} V_{xy}^{\vec{l}\,\vec{l}'} U_x^{\vec{l}} U_y^{\vec{l}'} . \tag{5}$$

$P_{x,y}^{\vec{l}}$ and $U_{x,y}^{\vec{l}}$ are the momentums and displacements of particles at

$$\vec{R}_x^{\vec{l}} = \vec{l}a + \{\tfrac{1}{2}a, 0\} + \{U_x^{\vec{l}}, 0\} , \qquad \vec{R}_y^{\vec{l}} = \vec{l}a + \{a, \tfrac{1}{2}a\} + \{0, U_y^{\vec{l}}\} , \tag{6}$$

indicating that the motion of the particles is subjected to the constraints shown in Fig. 1. Owing to these constraints, a particle can only displace either in the x or y direction.

The model Hamiltonian may be understood,[9] if one considers the situation of a crystal consisting of two sublattices. The atoms of one sublattice give rise to a short-range intracell anharmonic potential V_s, in which the atoms of the second sublattice, which we consider explicitly, move. These latter atoms are then coupled by means of a harmonic nearest-neighbor interaction V_I.

To determine the equilibrium position of the particles at $T = 0$ within the framework of classical mechanics, we consider

$$\frac{\partial}{\partial U_x^{\vec{l}}} V = A U_x^{\vec{l}} + B(U_x^{\vec{l}})^3 + \sum_{\vec{l}'} V_{xy}^{\vec{l}\,\vec{l}'} U_y^{\vec{l}'} \qquad \frac{\partial}{\partial U_y^{\vec{l}}} V = A U_y^{\vec{l}} + B(U_y^{\vec{l}})^3 + \sum_{\vec{l}'} V_{xy}^{\vec{l}\,\vec{l}'} U_x^{\vec{l}'} . \tag{7}$$

Next we impose the following additional constraints: (i) antiferrodistortive displacements, so that

$$U_x^{\vec{l}'} = U_x^{\vec{l}}(-1)^{l_x - l_x' + l_y - l_y'} ; \tag{8}$$

(ii) $V_{xy}^{\vec{l}\,\vec{l}'}$ [Eq. (5)] represents an isotropic nearest-neighbor interaction.

From these constraints it follows that (Fig. 1)

$$V_{xy}^{\vec{1}\,\vec{1}} = - V_{xy}^{\vec{1}\,\vec{2}} = V_{xy}^{\vec{1}\,\vec{3}} = - V_{xy}^{\vec{1}\,\vec{4}} = - C . \tag{9}$$

C designates the strength of the nearest-neighbor pair interaction. A, B, and C appearing in the potential energy [Eqs. (4), (5), and (9)] are the model parameters. Substituting relation (9) into (7), and setting these forces equal to zero, we find that at $T = 0$

$$(U_x^{\vec{l}})^2 = (U_y^{\vec{l}})^2 = (4C - A)/B . \tag{10}$$

This displacement corresponds to the local zero-temperature order parameter. To guarantee mechanical stability, the matrix

$$\left(\frac{\partial^2}{\partial U_x^{\vec{l}}\, \partial U_y^{\vec{l}'}} V\right) \tag{11}$$

must be positive definite. This requirement leads to the following condition:

$$4C - A > 0. \tag{12}$$

To guarantee that the antiferrodistortive low-temperature phase exists and leads to an absolute minimum of the potential energy, the parameter C [Eq. (9)], must be positive,

$$C > 0 , \tag{13}$$

and, moreover,

$$(U_x^{\vec{l}})^2 = (U_y^{\vec{l}}) = (4C - A)/B > 0 , \tag{14}$$

so that the local order parameter does not vanish at $T = 0$. The model parameter must then be chosen in such a way that conditions (12)–(14) are satisfied.

The arrangement of the atoms in the antiferrodistortive low-temperature phase is sketched in Fig. 2. It corresponds to the arrangement of the oxygen atoms in $SrTiO_3$ in the a-b plane.

The antiferrodistortive-phase transitions, associated with Hamiltonian (1) may be subdivided into two regimes,[8,9] according to the form of the single-particle potential in V_s [Eq. (4)]. The choice

$$A < 0 , \quad B > 0 , \quad C > 0 , \tag{15}$$

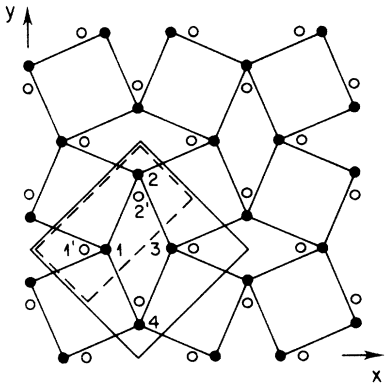

FIG. 2. Arrangement of the particles in the low- and high-temperature phases. Open circles form the reference lattice which is equivalent to that of the high-temperature phase, with atoms 1′ and 2′ per unit cell. Closed circles denote the positions of the particles in the low-temperature phase with four atoms per unit cell. Particle 1′ displaces only in the x direction, and particle 2′ in the y direction, whereas particles 1 and 3 displace in the x direction, and 2 and 4 in the y direction.

leads to a double-well single-particle potential implying antiferrodistortive transitions of the order-disorder type. In the displacive regime, the single-particle potentials in V_s [Eq. (4)] have a single minimum, implying both A and B positive, so that

$$A>0\,,\quad B>0\,,\quad C>0\,. \tag{16}$$

In the displacive regime, the low-temperature phase is stabilized by the pair interaction only [see Eq. (14)], whereas in the order-disorder regime, both the interaction term and the negative harmonic term ($A<0$) stabilize. Figure 3 shows schematically the two regimes and their limits. The Ising limit is reached if the wells are so steep that the motion within each can be neglected. In this case, Hamiltonian(1) reduces to the two-dimensional Ising Hamiltonian, representing a typical order-disorder model. In the displacive limit, we no longer have a low-temperature phase because the local order parameter [Eq. (14)] vanishes at $T=0$.

Emphasizing again that model Hamiltonian(1) goes over to the Ising one by changing the model parameter A continuously, it appears, by invoking the universality hypothesis, that the critical exponents associated with this Hamiltonian are expected to be close to those of the two-dimensional Ising model. A recent molecular-dynamics[1,2] investigation confirms this expectation.

III. ONE-PARTICLE DISPLACEMENT-PROBABILITY DISTRIBUTION

In the present section, we shall be concerned with a mathematical formalism, developed in the context of the theory of classical liquids,[7] which constitutes a convenient basis to investigate the properties of the one-, two-, and multi-particle displacement-probability distributions.

We consider the model system defined in Sec. II. This system is assumed to be in equilibrium and isothermal. Let us designate with

$$F_N(U_x^{\vec{1}}, U_y^{\vec{1}}, \ldots, U_x^{\vec{N}}, U_y^{\vec{N}}) = (1/Q)\, e^{-\beta V(\{U_x^{\vec{l}}, U_y^{\vec{l}}\})}, \tag{17}$$

where

$$Q = L^{-2N}\int_{-\infty}^{+\infty}\prod_{\vec{l}=\vec{1}}^{\vec{N}} dU_x^{\vec{l}}\,dU_y^{\vec{l}} \times e^{-\beta V(\{U_x^{\vec{l}}, U_y^{\vec{l}}\})}, \tag{18}$$

as the probability of finding the particles of $\{U_x^{\vec{l}}, U_y^{\vec{l}}\}$. This probability just equals the configurational part of the Gibbs' distribution function.[7] With the aid of this probability, we may then form

$$F_1(U_x^{\vec{1}}) = L^{-2N+1}\int dU_y^{\vec{1}}\prod_{\vec{l}=\vec{2}}^{\vec{N}} dU_x^{\vec{l}}\,dU_y^{\vec{l}} \times F_N(\{U_x^{\vec{l}}, U_y^{\vec{l}}\})\,, \tag{19}$$

$$F_2(U_x^{\vec{1}}, U_y^{\vec{1}}) = L^{-2N+2}\int\prod_{\vec{l}=\vec{2}}^{\vec{N}} dU_x^{\vec{l}}\,dU_y^{\vec{l}} \times F_N(\{U_x^{\vec{l}}, U_y^{\vec{l}}\})\,, \tag{20}$$

and higher-order correlation functions. $F_1(U_x^{\vec{1}})$ is the probability of finding the particle $(\vec{1}, x)$ at $U_x^{\vec{1}}$, with all remaining particles in arbitrary positions.

Of particular interest in this context is the sin-

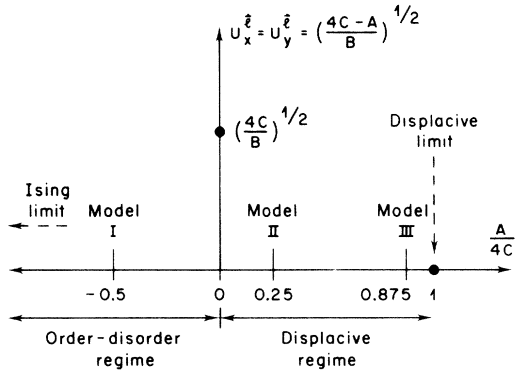

FIG. 3. Sketch of the order-disorder and displacive regime, including their limits for antiferrodistortive transitions. $U_x^{\vec{1}} = U_x^{\vec{1}} = [(4C-A)/B]^{1/2}$ [Eq. (10)] is the local order parameter at $T=0$. It vanishes in the displacive limit. The ratios $A/4C=-0.5$, 0.25, and 0.875 designate models I, II, and III, respectively, subsequently studied.

gle-particle correlation function $F_1(U_x^{\vec{1}})$, or the one-particle displacement-probability distribution. In fact, Müller and Berlinger[6] have shown that this quantity is related to the line shape of the electron-paramagnetic-resonance (EPR) absorption line, due to, for example, the iron–oxygen-vacancy ($Fe^{3+} - V_O$) pair centers, statistically distributed in the system. Due to this statistical distribution, the line shape is actually not proportional to $F_1(U_x^{\vec{1}})$ but to the symmetrical analog

$$\tilde{F}_1(U_x^{\vec{1}}) = \tfrac{1}{2}[F_1(U_x^{\vec{1}}) + F_1(-U_x^{\vec{1}})] , \tag{21}$$

the symmetrized one-particle displacement-probability distribution.

Next we derive some properties of $F_1(U_x^{\vec{1}})$. From the definition of the local order parameter

$$\langle U_x^{\vec{1}} \rangle = L^{-1} \int_{-\infty}^{+\infty} dU_x^{\vec{1}} (U_x^{\vec{1}}) F_1(U_x^{\vec{1}}) \tag{22}$$

and the fact that

$$\langle U_x^{\vec{1}} \rangle = 0 , \quad \text{for } T \geq T_c \tag{23}$$

we obtain

$$F_1(U_x^{\vec{1}}) = F_1(-U_x^{\vec{1}}), \quad \text{for } T \geq T_c \tag{24}$$

and

$$\frac{d}{dU_x^{\vec{1}}} F_1(U_x^{\vec{1}}) \bigg|_{U_{x=0}^{\vec{1}}} = -\frac{d}{dU_x^{\vec{1}}} F_1(-U_x^{\vec{1}}) \bigg|_{U_{x=0}^{\vec{1}}} = 0 \tag{25}$$

for $T \geq T_c$, so that according to Eqs. (21) and (24),

$$F_1(U_x^{\vec{1}}) = \tilde{F}_1(U_x^{\vec{1}}), \quad \text{for } T \geq T_c . \tag{26}$$

Moreover, it follows from relation (25) that $F_1(U_x^{\vec{1}} = 0)$ is extremum above T_c. The main motivation for the present investigation was the question whether or not this extremum is a minimum or a maximum and to what extent this property depends on the model parameters (A, B, C; Sec. II) chosen. The EPR measurements indicated[6] that, at least in $SrTiO_3$, $F_1(U_x^{\vec{1}} = 0)$ is maximum and single peaked above T_c.

To investigate this question for our model system, we next study the predictions of the Hartree approximation.

IV. PREDICTIONS OF HARTREE APPROXIMATION

In the Hartree approximation, one assumes

$$F_N(U_x^{\vec{1}}, U_y^{\vec{1}}, \ldots, U_x^{\vec{N}}, U_y^{\vec{N}}) = \prod_{1=\vec{1}}^{\vec{N}} F_1(U_x^{\vec{1}}) F_1(U_y^{\vec{1}}) , \tag{27}$$

so that the one-particle displacement-probability distribution is given by

$$F_1(U_x^{\vec{1}}) = D \exp\{-\beta[\tfrac{1}{2}A(U_x^{\vec{1}})^2 + \tfrac{1}{4}B(U_x^{\vec{1}})^4 - 4C\langle U_x^{\vec{1}} \rangle U_x^{\vec{1}}]\} . \tag{28}$$

$$D = L^{-1} \int_{-\infty}^{+\infty} dU_x^{\vec{1}} \times \exp\{-\beta[\tfrac{1}{2}A(U_x^{\vec{1}})^2 + \tfrac{1}{4}B(U_x^{\vec{1}})^4 - 4C\langle U_x^{\vec{1}} \rangle U_x^{\vec{1}}]\} . \tag{29}$$

Below T_c ($\langle U_x^{\vec{1}} \rangle \neq 0$) we find from Eqs. (27) and (28) three extrema in $\tilde{F}_1(U_x^{\vec{1}})$ at

$$U_x^{\vec{1}} = 0 \quad \text{(minimum)} , \tag{30}$$

$$(U_x^{\vec{1}})^2 = (16\beta C^2 \langle U_x^{\vec{1}} \rangle - A)/B \quad \text{(maxima)} . \tag{31}$$

For small $\langle U_x^{\vec{1}} \rangle$ the maxima occur only if

$$16\beta C^2 \langle U_x^{\vec{1}} \rangle^2 > A . \tag{32}$$

For

$$16\beta C^2 \langle U_x^{\vec{1}} \rangle^2 < A , \tag{33}$$

we have, however, even below T_c, a single-peak structure centered around

$$U_x^{\vec{1}} = 0 \quad \text{(maximum)} . \tag{34}$$

Above T_c, we find from Eqs. (30) and (31),

$$U_x^{\vec{1}} = 0 \quad \text{(minimum)} \tag{35}$$

$$(U_x^{\vec{1}})^2 = -A/B \quad \text{(maxima)}. \tag{36}$$

These analyses lead to the following predictions of the Hartree approximation: (a) Order-disorder regime (Fig. 3): $\tilde{F}_1(U_x^{\vec{1}})$ exhibits, above and below T_c, a double-peak structure as shown schematically in Fig. 4(a). (b) In the displacive regime (Fig. 3), and low temperatures, we have again a double-peak structure as long as condition (32) is satisfied [Fig. 4(b)]. By approaching T_c from below, however, $\langle U_x^{\vec{1}} \rangle$ decreases and at the same temperature $T^* < T_c$, condition (32), guaranteeing a double-peak structure can no longer be satisfied. At this temperature T^*, given by

$$16\beta C^2 \langle U_x^{\vec{1}} \rangle^2 = A , \tag{37}$$

the double-peak structure disappears. Above T^*, condition (33) applies, guaranteeing a single-peak structure centered at $U_x^{\vec{1}} = 0$ and persisting for all temperatures $T > T^*$ including T_c.

From these predictions, it follows that in the displacive regime the ratio

$$a_s = \left(\frac{d}{dU_x^{\vec{1}}} \tilde{F}_1(U_x^{\vec{1}})\right)_{\max} \Big/ \left(\frac{d}{dU_x^{\vec{1}}} \tilde{F}_1(U_x^{\vec{1}})\right)_{\min} \tag{38}$$

diverges at $T^* (< T_c)$ [Eq. (37)], because the denominator vanishes, [Eqs. (33), (34), and (37)]. This prediction, obtained within the framework of the Hartree approximation, is consistent with the EPR study by Müller and Berlinger[6] in $SrTiO_3$, where the existence of this divergence has been

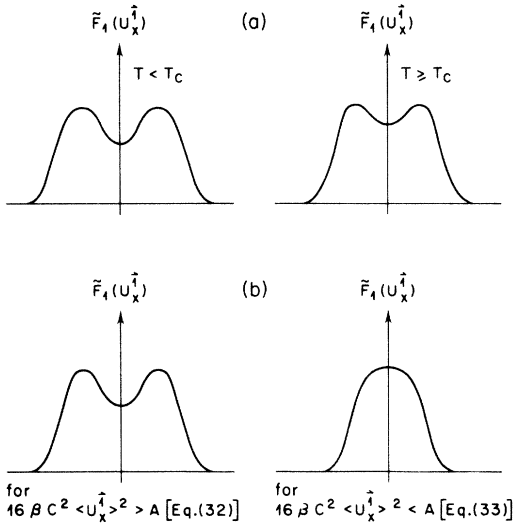

FIG. 4. Schematic sketch of the probability distribution $\tilde{F}_1(U_x^{\vec{1}})$ [Eq. (21)] according to the predictions of the Hartree approximation: (a) order-disorder regime; (b) displacive regime.

demonstrated for the first time. Within the framework of the Hartree approximation, however, the divergence of ratio (38) is uncritical in nature because it occurs at T^*, being—according to relation (37)—below T_c. In $SrTiO_3$, however, the divergence was found to occur rather close and presumably at T_c.[6]

For temperatures $T \geq T^*$, including T_c, the Hartree approximation predicts a single-peaked $\tilde{F}_1(U_x^{\vec{1}})$. A convenient method to test this prediction is the high-temperature expansion performed in Sec. V.

V. HIGH-TEMPERATURE EXPANSION RESULTS

It is evident that at high temperatures, the interaction term V_1 [Eq. (5)] is no longer of particular importance. In this temperature regime, we may expand therefore $e^{-\beta V}$ appearing in the configurational part of the Gibbs' distribution function [Eq. (17)] as follows:

$$e^{-\beta V} = e^{-\beta V_s}(1 - \beta V_I + \tfrac{1}{2}\beta^2 V_I^2 - \cdots + \cdots -) , \quad (39)$$

where V_s denotes the sum of the single-particle potentials given by Eq. (4).

Using this expansion, we next investigate the prediction of the Hartree approximation (Sec. IV), according to which $F_1(U_x^{\vec{1}})$ should exhibit a single-peaked structure for $T > T_c$, centered at $U_x^{\vec{1}} = 0$, so that

$$\left(\frac{d}{dU_x^{\vec{1}}} F_1(U_x^{\vec{1}})\right)_{U_x^{\vec{1}}=0} = 0 , \quad (40)$$

and

$$\left(\frac{d^2}{d(U_x^{\vec{1}})^2} F_1(U_x^{\vec{1}})\right)_{U_x^{\vec{1}}=0} < 0 . \quad (41)$$

Since (40) holds exactly for $T \geq T_c$, Eq. (25), we only have to study prediction (41). Using the definitions (17)–(19) and (5), we obtain the exact result:

$$\left(\frac{d^2}{d(U_x^{\vec{1}})^2} F_1(U_x^{\vec{1}})\right)_{U_x^{\vec{1}}=0} = -\beta A F_1(U_x^{\vec{1}}=0) + \frac{L^{-2N+1}}{Q}\beta^2 \int dU_y^{\vec{1}} \prod_{1=2}^{\vec{N}} dU_x^{\vec{1}} dU_y^{\vec{1}}$$
$$\times \left(\sum_{1'} V_{xy}^{\vec{1}\vec{1}'} U_y^{\vec{1}'}\right)^2 e^{-\beta V} = -\beta A F_1(U_x^{\vec{1}}=0) + \beta^2 C^2 G(U_x^{\vec{1}}=0) , \quad (42)$$

where, using Eq. (9),

$$G(U_x^{\vec{1}}=0) = (4/L)\int dU_y^{\vec{1}} (U_y^{\vec{1}})^2 F_2(U_x^{\vec{1}}=0, U_y^{\vec{1}}) + (4/L^2)\int dU_y^{\vec{1}} dU_y^{\vec{3}} U_y^{\vec{1}} U_y^{\vec{3}} F_3(U_x^{\vec{1}}=0, U_y^{\vec{1}}, U_y^{\vec{3}})$$
$$- (8/L^2)\int dU_y^{\vec{1}} dU_y^{\vec{2}} U_y^{\vec{1}} U_y^{\vec{2}} F_3(U_x^{\vec{1}}=0, U_y^{\vec{1}}, U_y^{\vec{2}}) . \quad (43)$$

The pair-correlation function $F_2(U_x^{\vec{1}}=0, U_y^{\vec{1}})$ is defined by Eq. (19) and the triplet correlation function, analogously by

$$F_3(U_x^{\vec{1}}, U_y^{\vec{1}}, U_y^{\vec{3}}) = L^{-2N+3}\int dU_x^{\vec{2}} dU_y^{\vec{2}} dU_x^{\vec{3}} \prod_{1=4}^{\vec{N}} dU_x^{\vec{1}} dU_y^{\vec{1}} F_N^{\vec{1}}(\{U_x^{\vec{1}}, U_y^{\vec{1}}\}) . \quad (44)$$

It is interesting to compare the exact expression (42) with the corresponding Hartree result. From Eq. (28), we obtain in this approximation

$$\left(\frac{d}{d(U_x^{\vec{1}})^2} F_1(U_x^{\vec{1}})\right)_{U_x^{\vec{1}}=0} = \frac{1}{D}(-\beta A + 16\beta^2 C^2 \langle U_x^{\vec{1}} \rangle^2) . \quad (45)$$

Comparing relations (43) and (45), it is seen that the first terms on the right-hand side have the same structure and do not vanish. The second term, however, vanishes in the Hartree expression (45) above T_c, so that $F_1(U_x^{\vec{1}})$ exhibits a single-peak structure centered at $U_x^{\vec{1}}=0$. In the exact expression, however, the second term is not expected to vanish, even above T_c. In fact, from spatial inversion it follows that

$$F_2(U_x^{\vec{1}}, U_y^{\vec{1}}) = F_2(-U_x^{\vec{1}}, -U_y^{\vec{1}}) , \tag{46}$$

and, in particular,

$$F_2(U_x^{\vec{1}}=0, U_y^{\vec{1}}) = F_2(U_x^{\vec{1}}=0, U_y^{\vec{1}}) . \tag{47}$$

These properties indicate that the first term in $G(U_x^{\vec{1}}=0)$ [Eq. (43)] may not vanish above T_c, as predicted by the Hartree approximation. We may suppose, therefore, that

$$\left(\frac{d^2}{d(U_x^{\vec{1}})^2} F_1(U_x^{\vec{1}})\right)_{U_x^{\vec{1}}=0} = -\beta A F_1(U_x^{\vec{1}}=0) + \beta^2 C^2 G(U_x^{\vec{1}}=0) > 0 , \tag{48}$$

leading to a double-peak structure of $F_1(U_x^{\vec{1}})$ with a minimum at $U_x^{\vec{1}}=0$, even above T_c. This double-peak structure will disappear at temperature T^*, defined by

$$-AF_1(U_x^{\vec{1}}=0) + \beta C^2 G(U_x^{\vec{1}}=0) = 0 , \tag{49}$$

at which a single-peak structure appears. Relation (49) is the exact analog to the Hartree condition (37).

To substantiate the conjecture, strongly violating the prediction of the Hartree approximation, that a double-peak structure in $F_1(U_x^{\vec{1}})$ might appear even above T_c, we next perform a high-temperature expansion of expression (42). In lowest order where, according to Eq. (39),

$$e^{-\beta V} \approx e^{-\beta V_s} ,$$

we obtain from relation (42)

$$\left(\frac{d^2}{d(U_x^{\vec{1}})^2} F_1(U_x^{\vec{1}})\right)_{U_x^{\vec{1}}=0} = -\beta\left(L \Big/ \int_{-\infty}^{+\infty} dU_x^{\vec{1}} e^{-\beta V_s(U_x^{\vec{1}})}\right) \times\left[A - 4BC^2\left(\int_{-\infty}^{+\infty} dU_x^{\vec{1}} (U_x^{\vec{1}})^2 e^{-\beta V_s(U_x^{\vec{1}})} \Big/ \int_{-\infty}^{+\infty} dU_x^{\vec{1}} e^{-\beta V_s(U_x^{\vec{1}})}\right)\right] , \tag{50}$$

where

$$e^{-\beta V_s(U_x^{\vec{1}})} = \exp\{-\beta[\tfrac{1}{2}A(U_x^{\vec{1}})^2 + \tfrac{1}{4}B(U_x^{\vec{1}})^4]\} . \tag{51}$$

In this order, only the first term in Eq. (43) contributes. Nevertheless, this lowest-order result already indicates that even at high temperatures the expression (50) might become positive so that

$$4\beta C^2 G^0(U_x^{\vec{1}}=0) > A , \tag{52}$$

where

$$G^0(U_x^{\vec{1}}=0) = \int_{-\infty}^{+\infty} dU_x^{\vec{1}} (U_x^{\vec{1}})^2 e^{-\beta V_s(U_x^{\vec{1}})} \Big/ \int_{-\infty}^{+\infty} dU_x^{\vec{1}} e^{-\beta V_s(U_x^{\vec{1}})} . \tag{53}$$

Provided that relation (52) can be satisfied, $F_1(U_x^{\vec{1}})$ will exhibit, even at high temperatures, a double-peak structure with a minimum at $U_x^{\vec{1}}=0$. To investigate this possibility, we evaluated $G^0(U_x^{\vec{1}}=0)$ numerically for various temperatures and the following two displacive models:

$$\text{Model II: } A=\tfrac{1}{2},\ B=\tfrac{1}{3},\ C=\tfrac{1}{2},\ A/4C=\tfrac{1}{4} ; \tag{54}$$

$$\text{Model III: } A=\tfrac{7}{4},\ B=\tfrac{1}{3},\ C=\tfrac{1}{2},\ A/4C=\tfrac{7}{8} . \tag{55}$$

We note that the units of time and length are chosen in such a way that the units of A, B, C, and k_BT are equal to one. The results are summarized in Tables I and II. In model II, being far from the displacive limit (Fig. 3), the lowest-order expansion results indicate (Table I), in conjunction with condition (52), that below $k_BT^*=4$, $F_1(U_x^{\vec{1}})$ will exhibit a double-peak structure with a minimum centered at $U_x^{\vec{1}}=0$. Noting that $k_BT_c=2.19$, this phenomenon is expected to occur even above T_c. In model III, which is rather close to the displacive limit, the expansion results, summarized in Table II suggest that condition (52) cannot be satisfied above $k_BT_c=0.245$. The expansion results indicate,

TABLE I. Numerical values for the factors appearing in relation (52), for model II, with parameters $A=\frac{1}{2}$, $B=\frac{1}{3}$, and $C=\frac{1}{2}$. In this displacive model we found, by means of the molecular-dynamics technique, $k_BT_c \approx 2.19$ [Eq. (56)].

k_BT	$G^0(U_x^{\vec{1}}=0)$	$4\beta C^2 G^0(U_x^{\vec{1}}=0)$	A
10	3.325	0.3325	0.5
8	2.938	0.3673	
6	2.499	0.4170	
4	1.980	0.4950	
3.907	1.953	0.5000	
3.500	1.832	0.5230	
3	1.673	0.5580	

TABLE II. Numerical values for the factors appearing in relation (52), for model III, with parameters $A=\frac{7}{4}$, $B=\frac{1}{3}$, and $C=\frac{1}{2}$. This model is rather close to the displacive limit (Fig. 3) because $4C-A=0.25$. A molecular-dynamics investigation indicates that $k_BT_c \approx 0.245$ [Eq. (57)].

k_BT	$G^0(\vec{U}_x=0)$	$4\beta C^2G^0(\vec{U}_x=0)$	A
3	1.111	0.370	1.75
2	0.813	0.407	
1	0.461	0.461	
0.5	0.252	0.504	
0.25	0.133	0.532	

therefore, that model III might exhibit a single-peak structure $\tilde{F}_1(\vec{U}_x)$ above T_c centered at $\vec{U}_x=0$.

From these estimates, it becomes clear that the shape of the one-particle probability distribution $F_1(\vec{U}_x)$ depends, above T_c, heavily on the ratio $A/4C$. In fact, the lowest-order expansion results, summarized in Tables I and II, indicate that T^*, designating the temperature at which the double-peak structure $\tilde{F}_1(\vec{U}_x)$ disappears, decreases by approaching the displacive limit.

By means of the high-temperature expansion technique, it is impossible however, to decide whether or not the double-peak structure disappears already at some temperature T^* below T_c, as predicted by the Hartree approximation [see Eq. (44)]. Nevertheless, using this technique, we have shown that a double-peak structure may even exist above T_c and that the changeover at T^* to a single-peak structure, and the associated divergence of ratio (38) is a noncritical phenomenon.

VI. MOLECULAR-DYNAMICS RESULTS

In the molecular-dynamics technique, the system is assumed to evolve according to Newton's equations associated with Hamiltonian (1). We considered, as in our previous work,[1,2] a system of 40×40 high-temperature unit cells (Fig. 2), subjected to periodic-boundary conditions. The particles are then allowed to move and their Canonical variables are calculated with a time increment. This set of difference equations approximates the set of Newton's equations. Explicit details of programming and the form chosen for the difference equations are given in the papers of Rahman[10] and Verlet.[11] For our purpose, however, it was more convenient to keep the temperature constant. This can be achieved by adjusting the instantaneous values of the velocities after any time increment in such a way that T remains fixed. In this procedure equilibrium is reached, while the instantaneous value of the order parameter, for example, fluctuates about a mean value. Using the equilibrium data saved one might then calculate space-time correlation functions, related to the linear response of the system, and time averages. The limitations of this technique as a tool to investigate phase transitions are similar to those of the Monte Carlo method. They have been discussed in that context extensively.[12]

Our data for the order parameter taken at various temperatures indicate that in the corresponding infinite system k_BT_c is close to

$$\text{Model II: } k_BT_c = 2.19; \tag{56}$$

$$\text{Model III: } k_BT_c = 0.245\ . \tag{57}$$

The critical exponents β and γ have been found to be consistent with those of the two-dimensional Ising model ($\beta=\frac{1}{8}$, $\gamma=\frac{7}{4}$), as expected from the universality hypothesis.[1,2]

Using the molecular-dynamics technique, we also calculated the symmetrized probability distribution $\tilde{F}_1(\vec{U}_x)$ [Eq. (38)] of the local displacements in models II and III at various temperatures. The results are plotted in Figs. 5 and 6. From Fig. 5, it is seen that model II [Eq. (54)], being rather far from the displacive limit $\tilde{F}_1(\vec{U}_x)$, exhibits a double-peak structure even above T_c. This result is consistent with the high-temperature expansion extimates (Table I) including temperature $k_BT^*=4$, at which the double-peak structure disappears. At this temperature ($k_BT^*=4>k_BT_c=2.19$) the ratio defined by Eq. (38) will of course diverge.

In model III, being rather close to the displacive limit (Fig. 3), the double-peak structure is seen to disappear (Fig. 6) around $k_BT^*\approx k_BT_c=0.245$. This result is consistent with the high-temperature expansion estimates (Table II) indicating that, for this model, $\tilde{F}_1(\vec{U}_x)$ might exhibit a single-peak structure only, above T_c.

From the molecular-dynamics results presented in this section, the following conclusions may be

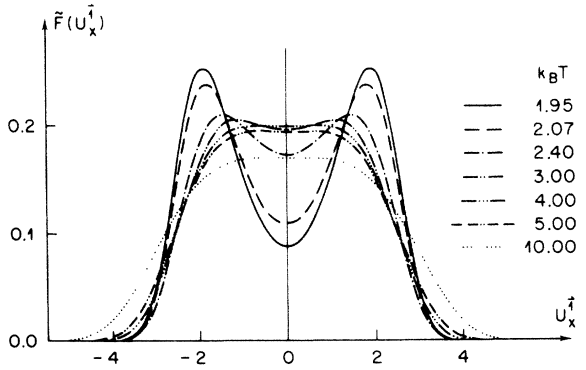

FIG. 5. Calculated probability distribution $\tilde{F}_1(\vec{U}_x)$ [Eq. (21)] in model II [Eq. (54)] at various temperatures k_BT. In this model k_BT_c is estimated to be $k_BT_c \approx 2.19$ [Eq. (56)].

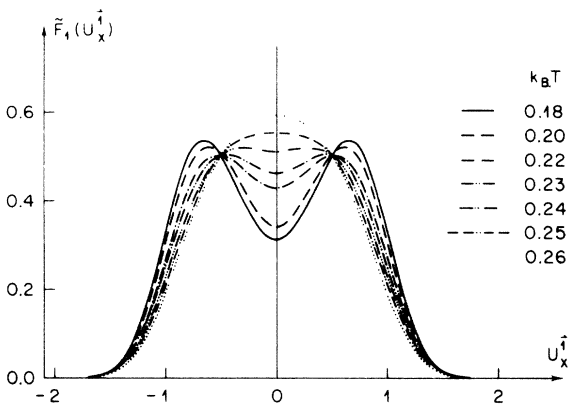

FIG. 6. Calculated probability distribution $\tilde{F}_1(U_x^{\vec{1}})$ [Eq. (21)] in model III [Eq. (55)] of various temperatures. We estimated k_BT_c to be $k_BT_c \approx 0.245$ [Eq. (57)].

drawn: (i) The double-peak structure of $\tilde{F}_1(U_x^{\vec{1}})$ may disappear above or close to T_c, depending for fixed B and C on the ratio $A/4C$. (ii) The ratio T^*/T_c, where T^* designates the temperature at which the double-peak structure disappears, or, equivalently, the temperature at which ratio (38) diverges, decreases by approaching the displacive limit with fixed B and C. In model II, we found $T^*/T_c = 1.8$ (Fig. 5) and in model III $T^*/T_c = 1$ (Fig. 6). (iii) These properties of $\tilde{F}_1(U_x^{\vec{1}})$ are consistent with the high-temperature estimates. (iv) From the present molecular-dynamics result, it is impossible, however, to draw a definite conclusion about a possible disappearance of the double-peak structure below $T_c (T^*/T_c < 1)$, as predicted by the Hartree approximation [Eq. (37)].

VII. SUMMARY AND CONCLUDING REMARKS

In this paper, we studied some properties of the one-particle displacement-probability distribution $F_1(U_x^{\vec{1}})$ and its symmetrized analog $\tilde{F}_1(U_x^{\vec{1}})$ by means of the Hartree approximation, a high-temperature expansion, and the molecular-dynamics technique.

Summarizing the main results, we first refer to Fig. 7. In the Ising limit (Fig. 3), the shape of $\tilde{F}_1(U_x^{\vec{1}})$ is qualitatively equal above and below T_c and consists of two symmetric δ spikes [Fig. 7(a)]. The ratio (38) is, in this limit, just a constant. By increasing A, with fixed B, for example, there is no dramatic change of this picture. At $T = 0$, we have again two symmetric δ spikes, broadening with increasing T [Fig. 7(b)]. For all finite temperatures, however, the double-peak structure persists. The ratio (38) increases with increasing temperature and diverges only at $T = -\infty$. This picture remains valid up to and including $A = 0$ [Eq. (52)] designating the boundary between the order-disorder and the displacive regime (Fig. 2). For $A \geq 0$, however, there is a temperature $T^* > T_c$, at which the double-peak structure of $\tilde{F}_1(U_x^{\vec{1}})$ goes over into a one-peak structure [Eq. (49)]. Here, the ratio (38) will diverge at $T = T^* > T_c$. This view has been confirmed by our high-temperature expansion analysis and by the molecular-dynamics results for model II. By increasing A further, T^* will decrease as the high-temperature expansion analysis and the molecular-dynamics study of model III revealed. At a particular ratio $A/4C$ for fixed B, T^* will coincide with T_c. The molecular-dynamics results for model III indicated that this ratio is close to $A/4C = \frac{7}{8}$ for $B = \frac{1}{3}$. The associated divergence of ratio (38) is, however, noncritical in nature, because it also occurs for such values of $A/4C$ where T^* differs from T_c. Close to the displacive limit ($A/4C \lesssim 1$) the symmetric δ spikes [Fig. 7(c)] become very close. Due to this fact, and the broadening of the spikes with increasing temperature, a single-peaked structure centered at $U_x^{\vec{1}} = 0$ is expected to appear at T^* below T_c. The molecular-dynamics results in model III support this possibility (Fig. 6), predicted by the Hartree approximation.

These results imply that the ratio T^*/T_c decreases with increasing ratio $A/4C$, as sketched in Fig. 8. For $A = 0$, T^* is infinite as might be seen from Eq. (52). The molecular-dynamics results in model III (Fig. 6) revealed, moreover, that T^*/T_c might become one for a particular ratio $A/4C$ with fixed B and C. Here, the divergence of ratio (38) might appear to be critical. Taking the model-parameter dependence of the ratio T^*/T_c into account, however, it becomes clear that this divergence is noncritical.

By increasing $A/4C$ further ($A/4C > 0.875$) we expect that the ratio T^*/T_c becomes smaller than one. Such behavior has been predicted by the Har-

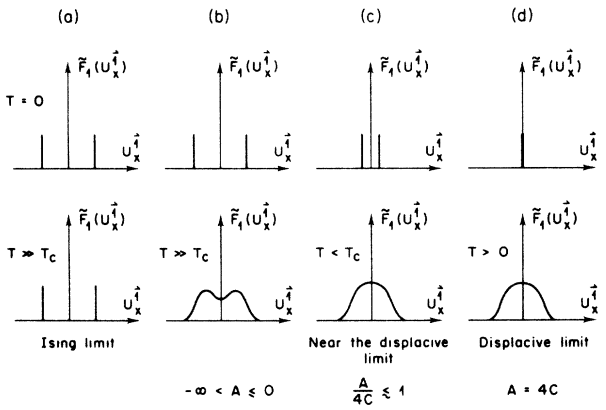

FIG. 7. Schematic sketch of the symmetrized probability distribution $\tilde{F}_1(U_x^{\vec{1}})$ [Eq. (21)] for various values of the ratio $A/4C$ by fixed B.

tree approximation [Eq. (37)]. To substantiate this conjecture, sketched in Fig. 8, we may go beyond the Hartree approximation. This may be achieved with the aid of the exact relation (42) and the approximations

$$F_2(U_x^{\vec{1}}=0, U_y^{\vec{1}}) = F_1(U_x^{\vec{1}}=0)\,F_1(U_y^{\vec{1}}) ,$$
$$F_3(U_x^{\vec{1}}=0, U_y^{\vec{1}}, U_y^{\vec{3}}) = F_1(U_x^{\vec{1}}=0)\,F_1(U_y^{\vec{1}})\,F_1(U_y^{\vec{3}}) . \quad (58)$$

Substituting Eq. (58) into Eqs. (42) and (43), we find

$$\left.\frac{d^2}{d(U_x^{\vec{1}})^2} F_1(U_x^{\vec{1}})\right|_{v_x^{\vec{1}}=0} = \left.\frac{d^2}{d(U_x^{\vec{1}})^2} \tilde{F}_1(U_x^{\vec{1}})\right|_{v_x^{\vec{1}}=0} = -\beta F_1(U_x^{\vec{1}}=0)\,[A - 4\beta C^2 \langle (U_x^{\vec{1}})^2\rangle - 12\beta C^2 \langle U_x^{\vec{1}}\rangle^2] , \quad (59)$$

where

$$\langle U_x^{\vec{1}}\rangle = \int dU_x^{\vec{1}} U_x^{\vec{1}} F_1(U_x^{\vec{1}}), \quad \langle (U_x^{\vec{1}})^2\rangle = \int dU_x^{\vec{1}} (U_x^{\vec{1}})^2 F_1(U_x^{\vec{1}}) . \quad (60)$$

This approximation differs from the Hartree one in that one starts from the exact expression for the second derivative and introduces, at this stage, a Hartree factorization. At low temperatures, where $\langle (U_x^{\vec{1}})^2\rangle \approx \langle U_x^{\vec{1}}\rangle^2$, relation (59) becomes identical to that of the Hartree approximation given by Eq. (45). As a consequence, relation (59) goes beyond the Hartree approximation and is expected to hold, therefore, also at temperatures $T \lesssim T_c$. In Table III, we listed estimates for the terms appearing in Eq. (59). It is seen that the second derivative (59) is predicted to become zero, below $T_c = 0.245$, at a temperature T^* ($0.24 < T^* \leq 0.245$), where the order parameter becomes sufficiently small. Recognizing that $\langle (U_x^{\vec{1}})^2\rangle$ decreases for fixed B and C as a function of the argument $A/4C$, it becomes clear that T^*/T_c will decrease further by increasing $A/4C$ above $\frac{7}{8}$, because a larger local order parameter $\langle U_x^{\vec{1}}\rangle$ is needed to cancel A in Eq. (59).

This behavior may be further substantiated by considering the dependence of the exact expression for T^*[Eq. (48)] on

$$\delta = 1 - A/4C . \quad (61)$$

Substituting this expression into Eq. (49) and noting that at low temperatures and small δ, $G(U_x^{\vec{1}}=0) \sim \delta$, whereas $F_1(U_x^{\vec{1}}=0)$ tends to a constant for $\delta = 0$, we find

$$T^* \sim \delta/(1-\delta) , \quad (62)$$

so that $T^* = \infty$ for $\delta = 1$ ($A = 0$) and in the displacive limit ($\delta = 0$) $T^* = 0$, as it should be. From the Hartree approximation, it is known that[13]

$$k_B T_c = (16C^2/3B)\,\delta , \quad (63)$$

close to the displacive limit, implying the general asymptotic behavior

$$T_c \sim \delta \quad (64)$$

as expected. Combining Eqs. (62) and (64) we find

$$T^*/T_c = k\,[1/(1-\delta)] , \quad (65)$$

close to the displacive limit. From the molecular-dynamics results for model III, we find $k \approx 0.875$, because $T^* \approx T_c$ and $1 - \delta = A/4C = 0.875$, so that T^*/T_c becomes smaller than one close to the displacive limit, as shown in Fig. 8.

Finally, at the displacive limit, we have at $T = 0$, a δ spike centered around $U_x^{\vec{1}} = 0$, because the order parameter vanishes [Fig. 7(d)]. Increasing temperature leads to a broadening of the δ function, but the single-peak structure persists for all temperatures.

To conclude, conclusive evidence has been given for the usefulness of the probability distribution $F_1(U_x^{\vec{1}})$ or its symmetrized analog $\tilde{F}_1(U_x^{\vec{1}})$ in elucidating the regime to which a particular antiferrodistortive transition belongs. Moreover, we have shown that the possible divergence of the ratio (38) is noncritical in nature. It may appear below, at or above T_c and is a property of the displacive regime. From Fig. 8, it is seen, however, that this property, which may be measured by the EPR

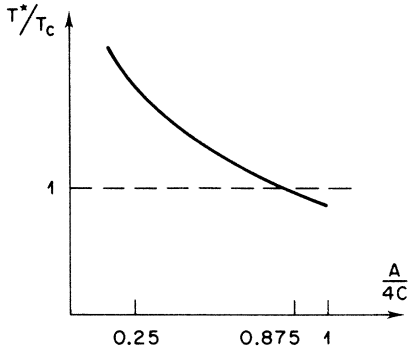

FIG. 8. Dependence of the ratio T^*/T_c on $A/4C$ for fixed B and C. T^* designates the temperature where ratio (38) diverges.

TABLE III. Numerical values for the terms appearing in relation (60), for model III, with parameters $A=\frac{7}{4}$, $B=\frac{1}{3}$, $C=\frac{1}{2}$, calculated with the molecular-dynamics technique.

k_BT	$\langle U_x^{\vec{I}}\rangle$	$\langle U_x^{\vec{I}}\rangle^2$	$\langle (U_x^{\vec{I}})^2\rangle$	$4\beta C^2[\langle (U_x^{\vec{I}})^2\rangle + 3\langle U_x^{\vec{I}}\rangle^2]$
0.18	0.57	0.32	0.48	9.78
0.20	0.56	0.31	0.47	7.00
0.22	0.48	0.23	0.43	5.09
0.23	0.43	0.18	0.41	4.13
0.24	0.35	0.12	0.38	3.08
0.26	0	0	0.34	1.31

technique,[6] may be used to determine the position of a particular system within the displacive regime. In fact, the ratio T^*/T_c, where T^* designates the temperature at which the ratio a_s[Eq. (38)] diverges, was found to depend on the model parameters chosen [(Fig. 8)]. In this case, we conclude that the experimentally verified divergence of ratio (38),[6] occurring in $SrTiO_3$ close to T_c or at T_c, corresponds to the special case $T^*/T_c \approx 1$, which we realized in model III, being close to the displacive limit. Our results have been derived, however, within the framework of classical statistical mechanics. As a consequence, we ignored the zero-point motions and the tunneling through the potential barrier ($A<0$). Koehler and Gillis[9] have taken into account these effects within the framework of the Hartree approximation. These authors have shown that even for $A<0$ (see Fig. 3), the double-peak structure of the one-particle distribution function might disappear already at some finite T^*, provided that the well of the particles is small enough. As a consequence, the boundary between the order-disorder and displacive regimes will be located at negative values of A, for any finite mass of the particles. This suggests that in those situations where quantum effects can no longer be neglected, the curve shown in Fig. 8 will be displaced to the left.

To conclude, we hope that our present work will prompt further EPR investigations of the symmetrized one-particle displacement-probability distribution, aiming to test our predictions. In fact, by means of the EPR technique, ratio (38) can be measured very accurately, close to T_c.[6]

ACKNOWLEDGMENTS

The authors are indebted to K. A. Müller, P. Meier, St. Sarbach, and H. Müller-Krumbhaar for valuable suggestions on this work.

[1]T. Schneider and E. Stoll, Phys. Rev. Lett. 31, 1254 (1973).
[2]T. Schneider and E. Stoll, in *Local Properties of Phase Transitions*, Proceedings of "Enrico Fermi" Summer School at Varenna, Italy, 1973 (Academic, New York, to be published).
[3]T. Riste, E. J. Samuelson, K. Otnes, and J. Feder, Solid State Commun. 9, 1455 (1971).
[4]S. M. Shapiro, J. D. Axe, G. Shirane, and T. Riste, Phys. Rev. B 6, 4332 (1972).
[5]Th. von Waldkirch, K. A. Müller, and W. Berlinger, Phys. Rev. Lett. 7, 1052 (1973).
[6]K. A. Müller and W. Berlinger, Phys. Rev. Lett. 29, 715 (1972).
[7]I. Z. Fisher, *Statistical Theory of Liquids* (University Press, Chicago, 1964).
[8]H. Thomas, in *Structural Phase Transitions and Soft Modes*, edited by E. J. Samuelson, E. Anderson, and J. Feder (Universitetsforlaget, Oslo, 1971), p. 15.
[9]T. R. Koehler and N. S. Gillis, Phys. Rev. B 7, 4980 (1973).
[10]A. Rahman, Phys. Rev. 136, A405 (1964).
[11]L. Verlet, Phys. Rev. 159, 98 (1967).
[12]E. Stoll, K. Binder, and T. Schneider, Phys. Rev. B 8, 3266 (1973).
[13]S. Sarbach, T. Schneider, and E. Stoll (unpublished).